Astronomy & Astrophysics

IRAS 18357-0604 – an analogue of the galactic yellow hypergiant IRC +10420?[⋆]

J. S. Clark[1], I. Negueruela[2], and C. González-Fernández[2,3]

[1] Department of Physics and Astronomy, The Open University, Walton Hall, Milton Keynes, MK7 6AA, UK
e-mail: s.clark@open.ac.uk
[2] Departamento de Física, Ingeniería de Sistemas y Teoría de la Señal, Universidad de Alicante, Apdo. 99, 03080 Alicante, Spain
[3] Institute of Astronomy, University of Cambridge, Madingly Road, Cambridge, CB3 0HA, UK

ABSTRACT

Context. Yellow hypergiants represent a short-lived evolutionary episode experienced by massive stars as they transit to and from a red supergiant phase. As such, their properties provide a critical test of stellar evolutionary theory, while recent observations unexpectedly suggest that a subset may explode as Type II supernovae.
Aims. The galactic yellow hypergiant IRC +10420 is a cornerstone system for understanding this phase since it is the strongest post-RSG candidate known, has demonstrated real-time evolution across the Hertzsprung-Russell diagram and been subject to extensive mass loss. In this paper we report on the discovery of a twin of IRC +10420 - IRAS 18357-0604.
Methods. Optical and near-IR spectroscopy are used to investigate the physical properties of IRAS 18357-0604 and also provide an estimate of its systemic velocity, while near- to mid-IR photometry probes the nature of its circumstellar environment.
Results. These observations reveal pronounced spectral similarities between IRAS 18357-0604 and IRC +10420, suggesting comparable temperatures and wind geometries. IR photometric data reveals a similarly dusty circumstellar environment, although historical mass loss appears to have been heavier in IRC +10420. The systemic velocity implies a distance compatible with the red supergiant-dominated complex at the base of the Scutum Crux arm; the resultant luminosity determination is consistent with a physical association but suggests a lower initial mass than inferred for IRC +10420 ($\lesssim$20 $M_\odot$ versus ~40 $M_\odot$). Evolutionary predictions for the physical properties of supernova progenitors derived from ~18–20 $M_\odot$ stars – or ~12–15 $M_\odot$ stars that have experienced enhanced mass loss as red supergiants – compare favourably with those of IRAS 18357-0604, which in turn appears to be similar to the the progenitor of SN2011dh; it may therefore provide an important insight into the nature of the apparently H-depleted yellow hypergiant progenitors of some Type IIb SNe.

Key words. stars: emission-line, Be – circumstellar matter – stars: evolution

1. Introduction

Yellow hypergiants (YHGs) are thought to represent a short lived episode of the post-main sequence (MS) evolution of massive stars; first encountered on a redwards passage across the Hertzsprung-Russell (HR) diagram and, for more massive stars, on a subsequent post-red supergiant (RSG) loop to higher temperatures. The precise mass range of stars that encounter this phase is a sensitive function of a number of stellar parameters such as initial mass and mass loss rate, rotational velocity and metalicity (e.g. Ekström et al. 2012), making their properties and population statistics critical tests of current stellar evolutionary theory. Moreover, with observational indications that YHGs drive extensive mass loss (transient rates $>10^{-4}$ $M_\odot$ yr^{-1}; Castro-Carrizo et al. 2007; Lobel et al. 2003) they may also play an important role in mediating the formation of Wolf-Rayet stars by stripping away the H-rich mantle of their progenitors.

Given this, it is unfortunate that YHGs are amongst the rarest sub-types of massive stars known, apparently reflecting the relative brevity of this evolutionary phase. De Jager (1998) and de Jager & Nieuwenhuijzen (1997) suggested that the most luminous YHGs are post-RSG stars on a blue loop across the HR diagram; unfortunately observationally identifying such objects has proved difficult. Oudmaijer et al. (2009) list three post-RSG stars – IRC +10420 (see also Jones et al. 1993), HD 179821 and RSGC1-F15 (cf. Davies et al. 2008), with a further three examples found in the literature – ρ Cas (Lobel et al. 2003), HD 8752 (Nieuwenhuijzen et al. 2012) and IRAS 17163-3907 (Lagadec et al. 2011). Of these, the most compelling case is provided by IRC +10420 due to a N-enriched chemistry, presence of a massive ejection nebula and apparent real time bluewards evolution across the HR diagram (Klochkova et al. 1997; Castro-Carrizo et al. 2007; Oudmaijer 1998). Currently demonstrating the earliest and richest emission line spectrum of any (candidate) galactic YHG as a result of its high luminosity, temperature and mass loss rate, it represents a cornerstone system for understanding the transition of stars away from the RSG phase to luminous blue variable (LBV), Wolf-Rayet (WR) or supernova (SN).

As part of an ongoing *I*-band spectroscopic survey of the environs of the RSG-dominated cluster complex/association at the base of the Scutum-Crux arm (RSG1-5; Figer et al. 2006; Davies et al. 2007a, 2008; Clark et al. 2009; Negueruela et al. 2010, 2011, 2012) we observed the bright but poorly studied IR source IRAS 18357-0604 (henceforth IRAS 1835−06; =2MASS J18382341-0601269) located 14′ from RSGC2/Stephenson 2, revealing an unusually rich emission line spectrum. With the optical region inaccessible due to high interstellar reddening,
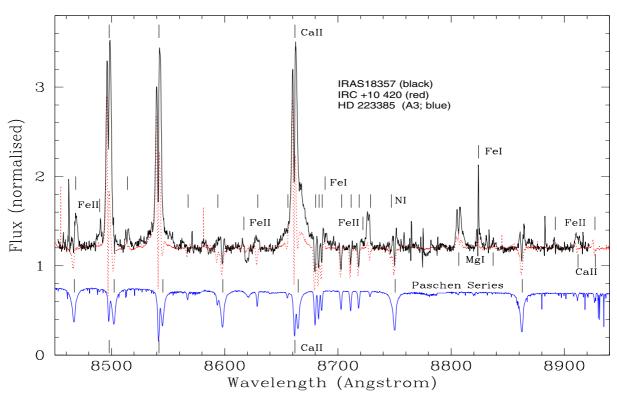
Fig. 1. *I* band spectrum of IRAS 1835−06 (black, solid lines) plotted against IRC +10420 (red, dotted) and HD 223385 (A3 Ia; blue, solid). Spectra have been shifted in wavelength to account for their individual systemic radial velocities as measured from the N Iλλ 8703.24, 8711.69, 8718.82 photospheric lines. Prominent emission and photospheric lines are indicated.

follow-up near-IR observations were made, which confirmed a striking similarity to IRC +10420; in the remainder of this paper we present and discuss these data and their implications.

2. Data acquisition and reduction

The *I*-band spectrum was obtained on the night of 2012 July 7 with the fibre-fed dual-beam AAOmega spectrograph on the 3.9 m Anglo-Australian Telescope (AAT) at the Australian Astronomical Observatory. The instrument was operated with the Two Degree Field ("2dF") multi-object system as front-end. Light is collected through an optical fibre with a projected diameter of 2″.1 on the sky and fed into the two arms via a dichroic beam-splitter with crossover at 5700 Å. Each arm of the AAOmega system is equipped with a 2k × 4k E2V CCD detector (the red arm CCD is a low-fringing type) and an AAO2 CCD controller. Due to the high reddening to the cluster and short exposure times, only the red arm registered usable spectra. The red arm was equipped with the 1700D grating, blazed at 10 000 Å. This grating provides a resolving power *R* = 10 000 over slightly more than 400 Å. The central wavelength was set at 8600 Å. The exact wavelength range observed for each spectrum depends on the position of the target in the 2dF field.

Data reduction was performed using the standard automatic reduction pipeline `2dfdr` as provided by the AAT at the time. Wavelength calibration was achieved with the observation of arc lamp spectra immediately before each target field. The lamps provide a complex spectrum of He+CuAr+FeAr+ThAr+CuNe. The arc line lists were revised and only those lines actually detected were given as input for `2dfdr`. This resulted in very good wavelength solutions, with rms always <0.1 pixels. Sky subtraction was carried out by means of a mean sky spectrum, obtained by averaging the spectra of 30 fibres located at known blank locations. The sky lines in each spectrum are evaluated and used to scale the mean sky spectrum prior to subtraction.

Near-IR spectra for IRAS 1835−06 were obtained on 2013 August 13 using LIRIS at the WHT telescope, as part of its service programme. As the source is very bright in this wavelength regime, we chose a narrow slit (0.65″) that, coupled with medium resolution grisms, yields an average resolving power around 3000 for the *J*, *H* and *K* bands. The data were taken using the standard scheme for near-IR observations, nodding the source along the slit in an ABBA pattern so to make it easy to remove sky emission when reducing the spectra. Said reduction was carried out in the standard fashion using the `lirisdr` package[1]. To correct for telluric absorption, a B9 star was observed alongside IRAS 18357-0604. Its spectrum was compared with an ATLAS model of the same spectral type, making sure that the differences around the prominent hydrogen absorption lines were low. The normalised ratio of the observed standard and the model was used then to correct our spectra. The selected B9 star, HIP091705, was chosen for its proximity to the target, yet it turned out to be an unresolved binary with a late type companion. This leaves some residuals when correcting for telluric absorption that show up as small CO emission bands, particularly for $\lambda > 2.3\ \mu$m. Consequently we do not discuss this region of the spectrum further.

The resultant spectra are presented in Figs. 1–3. For line identification in the *I*-band we relied on the detailed analysis of the spectrum of IRC +10420 by Oudmaijer (1998) supplemented by the study of the LBV Wd1-243 in an early-A spectral type phase by Ritchie et al. (2009). In the near-IR we utilised the
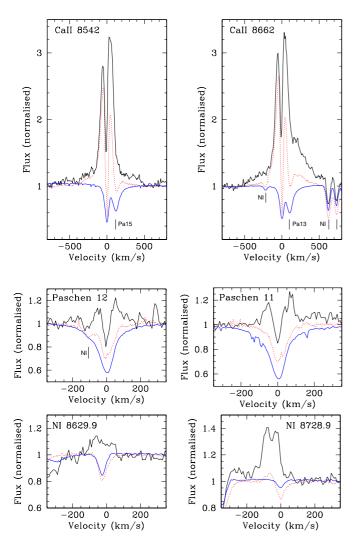

Fig. 2. Selected *I*-band transitions of the 3 spectra presented in Fig. 1 (IRAS 1835−06 – black, solid lines; IRC +10420 – red, dotted; HD 223385 – blue, solid). Spectra have been shifted in velocity to account for their individual systemic radial velocities as described in Fig. 1.

line lists for both IRC +10420 (Yamamuro et al. 2007) and other emission line stars (Hamann et al. 1994; Kelly et al. 1994; Clark et al. 1999; and Filliatre & Chaty 2004).

3. Results

As described earlier, the similarities between the *IJHK*-band spectra of IRAS 1835−06 and IRC +10420 (Oudmaijer 1998; Humphreys et al. 2002; Yamamuro et al. 2007; all obtained post transition to spectral type A2 Ia⁺) are particularly striking (Figs. 1 and 3). In both cases they are dominated by emission in the lower transitions of the Paschen and Brackett series as well as low excitation metallic species such as Fe I-II, Mg I, N I, Na I, Ti II and in particular Ca II. None of the higher excitation lines that are present in early, luminous stars (e.g. He I-II, C III-IV and N III) were seen in emission or absorption. The only photospheric absorption lines common to both stars were the N I transitions between ∼8670–8730 Å, with stronger emission in the higher Paschen series in IRAS 1835-06 masking the photospheric lines present in IRC +10420 (Figs. 1 and 2; see below).
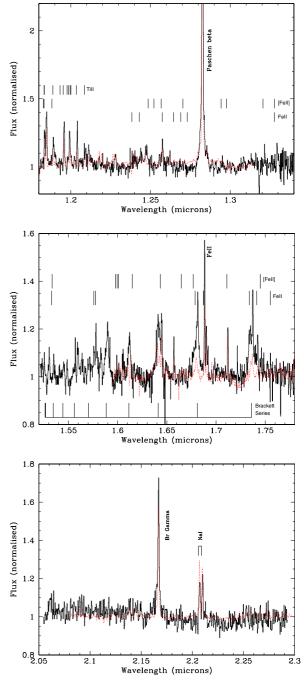

Fig. 3. *JHK*-band spectra of IRAS 1835−06 (black, solid lines) and IRC +10420 (red, dotted) with transitions due to the Paschen and Brackett series, Fe II, [Fe II], Na I and Ti II indicated. Peak intensity of the Paβ line is ∼5.2 and ∼3.4 times continuum for IRAS 1835−06 and IRC +10420 respectively. Spectra have been corrected for apparent radial velocity as described in Fig. 1.

Fortuitously, the strength of the N I absorption lines in the *I*-band can function as an approximate temperature diagnostic in late B to early F supergiants, becoming progressively stronger for cooler stars (e.g. Munari & Tomasella 1997; Clark et al. 2005). The efficacy of such an approach is shown by comparison of the N I lines in the spectrum of IRC +10420 to those of the A3 Iae (and candidate YHG) HD 223385; being marginally stronger and hence indicative of a slightly cooler star in the former. Such a classification is entirely consistent with that of early- to mid-A by Oudmaijer (1998) utilising the

~4700–4950 Å region of the same spectrum (and also that of Klochkova et al. 2002). Given that these transitions are weaker in IRAS 1835−06 one might infer a slightly earlier spectral type for it than IRC +10420 (~A0-2). This would also be consistent with the near-IR spectroscopic properties; the lack of He I 2.112 μm in absorption suggest $T < 10\,000$ K (or A0 or later; Clark et al. 2011), while cooler ($T \lesssim 7500$ K; spectral classes F-G) YHGs such as ρ Cas and HR8752 appear unable to support the Brackett series in emission (Yamamuro et al. 2007).

Turning to the emission component of the spectrum and such cool temperatures are fully consistent with the presence of both Mg I and strong Ca II emission which, given their ionisation potentials (7.65eV and 11.9eV respectively), likely arise in a neutral H I region (cf. Wd1-243; Ritchie et al. 2009). While emission in the Ca II lines is stronger in IRAS 1835-06 than IRC +10420, the profiles in both stars show a remarkable resemblance in both morphology and kinematics; comprising high velocity wings and a narrow, double peaked component (Fig. 2). Following IRC +10420, the emission in the high velocity wings of IRAS 1835-06 increases from Ca II 8498.02 Å, through 8542.09 Å to 8662.14 Å; furthermore the excess emission in the red over the blue wing of the latter transition in IRC +10420 is also replicated (Fig. 2). The high velocity emission wings are attributed to Thompson (electron) scattering in IRC +10 420 and such a process appears likely here too. However, unlike IRC +10420, the red peak is stronger than the blue in all three transitions in IRAS 1835−06. While emission is present in the (unblended) Pa11 and 12 lines of IRAS 1835−06 (Fig. 2; seen in absorption in IRC +10420), their modest strength suggests that it is unlikely that blending of Pa13, 15 and 16 with their adjacent Ca II lines could cause this reversal. Where unblended, the Paschen lines demonstrate the "shell-like" emission profile characteristic of a subset of classical Be stars (Sect. 4). Although hampered by the lower S/N observations, where they are discernable the trend to stronger emission in IRAS 1835−06 is also present in the remaining weak, low excitation metallic transitions, which also appear broader than in IRC +10420, with several appearing double peaked. A particularly notable feature of the IRC +10420 spectrum is the occurence of inverse P Cygni profiles in some of these lines (e.g. N Iλ8728.9 Å; Oudmaijer 1998, see also Humphreys et al. 2002) and a variant of this behaviour is also present in IRAS1835-06, where the pure (double peaked) emission component in this transition appears similarly blueshifted (Fig. 2).

Finally, we may estimate the apparent systemic velocity of IRAS 1835−06 from the N I$\lambda\lambda$8703.24, 8711.69, 8718.82 lines. Measurement of the systemic velocity shifts in these lines in the spectrum of IRC +10420 reveals a mean value of ~70 km s^{-1}; broadly consistent with that derived from CO rotational lines (75 km s^{-1}; Jones et al. 1993; Oudmaijer et al. 1996) and hence not subject to the anomalous redshift evident in some forbidden lines (10–20 km s^{-1}; Oudmaijer 1998). Consequently, we are reassured that the mean value for IRAS 1835−06 (~90 ± 3 km s^{-1}) reflects the true systemic velocity, noting a correction for transformation to the Local Standard of Reference (LSR) system in this direction of ~14 km s^{-1}. For comparison H II regions in the vicinity of Ste2 have $v_{LSR} \sim 90$ km s^{-1}, while cluster members have been identified in the range 100 km s$^{-1} \leq v_{LSR} \leq 120$ km s^{-1}, which includes velocity outliers such as Ste2-17 and Ste2-23 (Davies et al. 2007a; Negueruela et al. 2012). We therefore adopt the working hypothesis that IRAS 1835−06 is located at the same distance (~6 kpc) as Ste2 and associated star forming region for the remainder of this paper.

4. Discussion

4.1. Spectral comparisons

Given that YHGs, (cool phase) LBVs and supergiant B[e]/A[e] stars are co-located on the HR diagram and show similar spectral morphologies (dominated by emission in H I and low excitation metals), it is worth investigating whether IRAS 1835−06 fulfills the classification criteria of either of the latter two classes of star. *I*-band spectroscopy of LBVs shows a diversity of behaviour. During their cool-phases HR Car and AG Car show pronounced differences with respect to IRAS 1835−06; the spectrum of HR Car being characterised by weak P Cygni emission in the Paschen series, which are stronger and supplemented by N I emission in AG Car – in neither case is Ca II emission prominent (Machado et al. 2002; Jose Groh, priv. comm., 2013). Conversely, in systems where it is prominent, neither the Paschen series nor low excitation metal lines are in emission (e.g. S Dor & Wd1-243; Munari et al. 1997; Clark & Negueruela 2004).

Only two A[e] supergiants are known and only one – 3 Pup – has published *I*-band data. Ca II emission is present, although the line profiles are narrower than in IRAS 1835−06 and also lack a deep central absorption trough and strong emission wings (Chentsov et al. 2010). These differences are also present in these transitions in hotter B[e] supergiants (Aret et al. 2012). No systemic surveys of either LBVs or B[e]/A[e] supergiants are available in the *JH*-bands, but in the *K*-band both IRC +10420 and IRAS 1835−06 lack the weak Fe II and Mg II emission of the coolest LBVs (Clark et al. 2011), but demonstrate stronger Na I emission with respect to Brγ than seen in B[e] stars (Oksala et al. 2013).

We conclude that IRAS 1835−06 most closely resembles the YHG IRC +10420 in comparison with both LBVs and B[e]/A[e] supergiants, although we caution that these classifications are likely not mutually exclusive. For example the sgB[e] star S18 demonstrates LBV-like photometric and spectroscopic variability (Clark et al. 2013). Likewise the cool-phase spectrum of the LBVs R71 and R143 (Munari et al. 2009; Mehner et al. 2013) are almost indistinguishable from those of the YHGs Wd1-12 and 16a (Clark et al. 2005); in the absence of variability both R71 and R143 would have also been classified as YHGs. The contrast between the *I*-band spectra of IRC +10420 and IRAS 1835−06 (dominated by emission) and the YHGs within Westerlund 1 (dominated by absorption) also highlights an additional issue: the heterogeneous nature of YHG spectra, even for stars of similar temperature such as these four. Potential explanations for this diversity are the wide range of luminosities spanned by known examples (log($L_{bol}/L_\odot$) ~ 5.2−6.2; Sect. 4.2, Davies et al. 2008; Clark et al., in prep.)[2] and presence of both pre- and post-RSG examples, with the properties of the latter expected to be influenced by the chemical enrichment and substantial mass loss that they will have experienced.

The unusual emission line profiles that characterise the IRC +10420 spectrum have led to significant debate regarding the geometry of the circumstellar environment/wind (cf. Jones et al. 1993; Oudmaijer et al. 1996; Humphreys et al. 2002; Davies et al. 2007b). Recent interferometric observations suggested a mass loss rate of ~1.5−2 × 10^{-5} $M_\odot$ yr^{-1} and confirmed asphericity in the inner wind (Driebe et al. 2009), who suggested that either the wind was intrinsically asymmetric, with a greater mass loss from the hemisphere pointed towards us or that the

---

[2] Although in this case the luminosities of IRC +10420, Wd1-12 and 16a are expected to be broadly comparable (e.g. Oudmaijer et al. 2009).

wind is spherical, with emission from the receding component blocked by an equatorial disc. Subsequently Tiffany et al. (2010) suggested that IRC +10420 is observed in the pole-on orientation required by the latter hypothesis, with Oudmaijer & de Wit (2013) favouring a geometrical model in which the receding portion of a polar wind is occulted by the stellar disc, leading to the asymmetric Hα and Ca II lines.

It would therefore be natural to infer a similarly powerful, asymmetric wind for IRAS 1835−06, given its overal spectral similarity. However, the observed blue- to red-peak ratio of the Ca II lines in IRAS 1835−06 could not arise through obscuration/inclination effects (which should only act to reduce the strength of the red-shifted peak relative to blue) and so would have to reflect a real asymmetry in wind strengths between different hemispheres. Motivated by the shell-like lines in the Paschen series, an alternative explanation might be that both Ca II and Paschen series lines arise in an equatorial disc viewed "edge-on" (cf. *o* And; Clark et al. 2003). However, classical Be stars observed in such an orientation also demonstrate shell profiles in low-excitation metallic species such as Fe II; such behaviour is not reproduced in IRAS 1835−06.

4.2. IR properties

IRAS 1835−06 is a highly reddened system ($J = 8.54 \pm 0.02$, $H = 6.28 \pm 0.02$ and $K = 4.63 \pm 0.02$) for which no optical photometry is currently available. Adopting the intrinsic colour for an ∼A2 Ia star (($J − K$) ∼ 0.11; Koornneef 1983) leads to $E(J − K)$ ∼ 3.8; with an IR reddening-free parameter $Q_{IR} = (J − H) − 1.8 \times (H − K)$ ∼ −0.7 (Negueruela et al. 2012), suggesting a combination of both interstellar extinction and circumstellar emission. Such a conclusion is supported by its mid-IR luminosity; IRAS 1835−06 is saturated in GLIMPSE/*Spitzer* data (Benjamin et al. 2003) but is a bright point source apparently associated with no extended emission in IRAS (IRAS PSC 1985), Midcourse Source Experiment (Egan et al. 2001) and WISE (Wright et al. 2010) data[3]. Likewise Kwok et al. (1997) report a featureless low resolution IRAS spectrum that is flatter than expected for a stellar source.

Potential contamination of the near-IR photometry by dust emission renders a direct reddening determination unreliable. Consequently, given its proximity to Ste2 (Sect. 3) we make use of the mean reddening towards the cluster (A_K ∼ 1.0 ± 0.25; Froebrich & Scholz 2013). After dereddening these data (following Messineo et al. 2005) we may then determine the near/mid-IR colour indices employed by Davies et al. (2007a)[4], from which we find that IRAS 1835−06 supports a larger IR excess than any cluster member – including the post-RSG candidate Ste2-49 – confirming the presence of warm circumstellar dust (Fig. 4). Given the spectral similarities of IRAS 1835−06 and IRC +10420, if we assume both support comparable winds (Driebe et al. 2009) then following the analysis of Kochanek (2011) dust should not currently be able to condense in either system. This would imply that IRAS 1835−06 has recently undergone an episode of enhanced mass loss and it is tempting to suggest that it has just exited a RSG-phase during which the circumstellar dust formed. However, it appears to lack the massive,
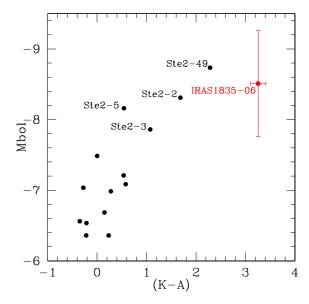

Fig. 4. ($K − A$) near- to mid-IR colour indice versus M_{bol} for IRAS 1835−06 and members of Ste2 (following Davies et al. 2007a). Errors in M_{bol} for IRAS 1835-06 are dominated by uncertainty in reddening and the value is for an assumed distance of ∼6 kpc. Individual errors for Ste2 members are not presented by Davies et al. (2007a, their Fig. 10) but appear to be ≲0.25 mag in M_{bol} and of order the symbol size in ($K − A$). In the absence of an IR excess we would expect a star to reside at ($K − A$) ∼ 0.

spatially resolved ejecta that characterises both IRC +10420 and IRAS 17163-3907 (1 $M_{\odot}$ and 4 $M_{\odot}$ respectively), although these are by no means ubiquitous amongst YHGs, being absent for ρ Cas and HR 8752 (Humphreys et al. 1997; Schuster et al. 2006; Castro-Carrizo et al. 2007; Lagadec et al. 2011).

Finally, using the mean cluster reddening and the *J*-band magnitude – since it is least likely to be contaminated by dust emission – we may estimate the current bolometric luminosity of IRAS 1835−06. Following Okumura et al. (2000) we may convert A_K to A_J and then for a distance modulus of 13.9 (∼6 kpc) we find M_J ∼ −8.3 ± 0.7. Then employing the colour relationships from Koornneef (1983) and the relevant bolometric correction for early A supergiants (Clark et al. 2005) we arrive at $\log(L_{bol}/L_{\odot})$ ∼5.2 ± 0.3, where the error quoted is dominated by uncertainties in the interstellar reddening. This value suggests that IRAS 1835−06 is intrinsically less luminous than IRC +10420 ($\log(L_{bol}/L_{\odot})$ ∼ 5.7–5.8; e.g. Jones et al. 1993, Oudmaijer et al. 1996) and hence also less massive (≲20 $M_{\odot}$ versus ∼40 $M_{\odot}$), noting that any contribution to the *J*-band flux by warm dust would lead to a corresponding reduction in luminosity.

4.3. Environmental and evolutionary context

Are the properties we adopt for IRAS 1835−06 consistent with a physical association with either Ste2 or the larger RSG agglomerate at the base of the Scutum-Crux arm (Sect. 1)? RSGC1 and Ste2 appears to be the youngest and oldest clusters within this complex, suggesting star formation peaking over the last 10–20 Myr resulting in M_{init} ∼ 12−22 $M_{\odot}$ for evolved stars within this region (Davies et al. 2008)[5]. If this age range

---

[3] WISE fluxes of $F_{3.35\,\mu m}$ ∼ $15.7^{+2.0}_{-1.8}$Jy, $F_{4.60\,\mu m}$ ∼ $38.3^{+4.7}_{-4.2}$ Jy, $F_{11.56\,\mu m}$ ∼ $19.7^{+1.0}_{-1.0}$ Jy and $F_{22.09\,\mu m}$ ∼ $18.5^{+0.3}_{-0.3}$ Jy, MSX fluxes of $F_{8.28\,\mu m}$ ∼ 27.3 ± 1.1 Jy, $F_{12.13\,\mu m}$ ∼ 27.7 ± 1.4 Jy, $F_{14.7\,\mu m}$ ∼ 24.5 ± 1.5 Jy and $F_{21.34\,\mu m}$ ∼ 18.0 ± 1.1 Jy and IRAS fluxes of $F_{12\,\mu m}$ ∼ 27 Jy, $F_{25\,\mu m}$ ∼ 19.1 Jy and $F_{60\,\mu m}$ ∼ 17.1 Jy.
[4] ($K − A$) ∼ 3.3, ($K − C$) ∼ 4.2 and ($K − D$) ∼ 3.6.

[5] An age of 12 ± 2 Myr and 17 ± 3 Myr for RSGC1 and Ste2 respectively, implying initial masses of 18^{+4}_{-2} $M_{\odot}$ and 14 ± 2 $M_{\odot}$ for the RSG cohorts.
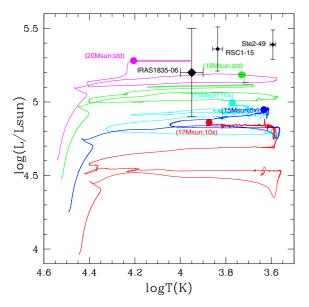
Fig. 5. HR diagram showing the position of IRAS 1835−06 and the post-RSG candidates RSGC1-15 and Ste2-49 (Davies et al. 2007a, 2008) assuming a distance of ~6 kpc. We conservatively adopt 8000 K < T < 10 000 K for IRAS 1835−06 (appropriate for an A hypergiant). We also plot the evolutionary tracks of Georgy (2012) and Groh et al. (2013b) with the positions of the resultant SNe indicated by coloured dots. The 18 $M_\odot$ and 20 $M_\odot$ tracks (green and purple respectively) assume the standard mass loss rate prescription of Ekström et al. (2012), the 15 $M_\odot$ tracks 5× and 10× standard (dark and light blue respectively) and the 12 $M_\odot$ track assumes a mass loss rate 10× standard (red).

is applicable to the wider RSG association then the current luminosity and temperature of IRAS 1835−06 are consistent with membership, with theoretical models for rotating stars with $M_{init} \sim 18$–20 $M_\odot$ reproducing its current parameters at an age comparable to that of RSGC1 (Fig. 5; Ekström et al. 2012; Groh et al. 2013b). This in turn would imply that IRAS 1835−06 could either be the *immediate* progenitor of a core-collapse Type IIb SN, or may instead evolve through an LBV phase prior to encountering this fate, with the $M_{init} \sim 18$ $M_\odot$ model terminating as a YHG ($T \sim 5400$ K) and the $M_{init} \sim 20$ $M_\odot$ terminating as a LBV ($T \sim 19\,500$ K), in concert bracketing the current properties of IRAS 1835−06.

More particularly, are the properties of IRAS 1835−06 consistent with an origin within, and subsequent ejection from, the older cluster Ste2[6]? Stars of such an age are not expected to evolve past the RSG phase and the current luminosity and temperature of IRAS 1835−06 are not consistent with a pre-RSG YHG phase (Ekström et al. 2012). However Davies et al. (2007a) identify Ste2-49 as a putative post-RSG object, while Ste2-2, 3 and 5 also have luminosities in excess of $\log (L_{bol}/L_\odot) \sim 5.0$; hence comparable to IRAS 1835−06. Moreover, all four of these stars support the most extreme mass loss rates of any of the members of Ste-2 (as measured from their dust-driven mid-IR excesses; Fig. 4) and hence it is tempting to posit that IRAS 1835−06 is a more evolved descendent of such stars.

Georgy (2012; Fig. 5) shows that an increase in the mass loss rates adopted for RSGs by a factor of 5–10 would enable stars in this mass range to evolve through to a YHG phase immediately

---

[6] Assuming a transverse "runaway" velocity of 10 km s^{-1} (compared to a 1σ velocity dispersion of ~3 km s^{-1} for Ste2; Davies et al. 2007a) would place IRAS 1835−06 14′ distant after only 730 000 yr; well within the expected lifetime of such a star.

prior to a SN endpoint, again with properties broadly comparable with those of IRAS 1835−06 (cf. their $M_{init} \sim 12(15)$ $M_\odot$ models with a mass loss rate 10× standard, which at SN have $\log (L_{bol}/L_\odot) \sim 4.87(5.0)$ and $T_{eff} \sim 7400(6000)$ K). Such stars would be expected to approach the Eddington limit and hence support strong current mass loss rates, implying that observationally they should resemble IRAS 1835−06 (Jose Groh, priv. comm. 2013).

Consequently, if the association of IRAS 1835−06 with Ste2 were confirmed it would validate the suggestion that (a subset of) RSGs experience extreme mass loss rates and as a result provide an unique insight into the properties of low luminosity yellow super-/hypergiant SNe progenitors such as that of the Type IIb event SN2011dh ($\log (L_{bol}/L_\odot) \sim 4.9 \pm 0.2$, $T_{eff} \sim 6000 \pm 200$ K and $M_{init} \sim 13 \pm 3$ $M_\odot$; Maund et al. 2011; van Dyk et al. 2013). Indeed, despite their relatively low luminosities, such SNe progenitors would better be classified as hypergiants rather than supergiants (as currently described in the literature), given their extreme post-RSG mass loss rates which would result in rich emission line spectra (cf. Groh et al. 2013b).

5. Conclusions

In spectroscopic terms IRAS 1835−06 is a near-twin of the hitherto unique post-RSG YHG IRC +10420. Similarly demonstrating asymmetric, twin-peaked emission line profiles – indicative of aspherical, outflowing material – IRAS 1835-06 reveals that the complex circumstellar environment of IRC +10420 is not a pathological case, but instead potentially represents a template for this phase of stellar evolution. The mid-IR properties of IRAS 1835−06 reveal the presence of a substantial dusty circumstellar component which, although apparently not as massive as that of IRC +10420, is fully consistent with identification as a YHG. Given that it appears unlikely that its current wind could support dust condensation, this is suggestive of a recent exit from a high mass loss rate episode (possibly associated with the preceding RSG phase).

A distance of ~6kpc is inferred from the systemic velocity of IRAS 1835−06, which would place it in the RSG "association" at the base of the Scutum-Crux arm. Such a distance implies $\log(L_{bol}/L_\odot) \sim 5.2 \pm 0.3$; entirely consistent with an origin in the same burst of star formation that yielded the RSG population (although we caution that such a value must be regarded as *provisional* pending a re-determination utilising deep optical observations that are free from contamination from circumstellar dust). Likewise its apparent rarity – the only known example in comparison to ~10^2 RSGs within the complex – is predicted by current evolutionary models (e.g. Ekström et al. 2012; Davies et al. 2009). Located 14′ from the massive cluster Ste2, identification as a runaway cannot be excluded, but an unexpectedly extreme mass-loss rate during the preceding RSG phase would be required to replicate its current properties in such a scenario.

Nevertheless, either scenario would imply that IRAS 1835−06 could represent the *immediate* progenitor of a core-collapse SN (Georgy 2012; Groh et al. 2013b) and its current physical properties are indeed similar to those of the YHG progenitor of SN2011dh. IRAS 1835−06 may therefore shed light on both the rapid, post-RSG evolution of massive stars and also the nature of the YHG progenitors of some Type IIP and IIb SNe (e.g. SN1993J, SN2008cn and SN2009kr; Maund et al. 2011), which are thought to arise from moderately massive stars which have been progressively stripped of their hydrogen mantle.

References

Aret, A., Kraus, M., Muratore, M. F., & Borges Fernandes, M. 2012, MNRAS, 423, 284
Benjamin, R. A., Churchwell, E., Babler, B. L., et al. 2003, PASP, 115, 953
Castro-Carrizo, A., Quintana-Lacaci, G. Bujarrabal, V., Neri, R., & Alcolea, J. 2007, A&A, 465, 457
Chentsov, E. L., Klochkova, V. G., & Miroshnichenko, A. S. 2010, Astrophys. Bull., 65, 150
Clark, J. S., & Negueruela, I. 2004, A&A, 413, L15
Clark, J. S., Steele, I. A., Fender, R. P., & Coe, M.J. 1999, A&A, 348, 888
Clark, J. S., Tarasov, A. E., & Panko, E. A., 2003, A&A, 403, 239
Clark, J. S., Negueruela, I., Crowther, P. A., & Goodwin, S. P. 2005, A&A, 434, 949
Clark, J. S., Negueruela, I., Davies, B., et al. 2009, A&A, 498, 109
Clark, J. S., Arkharov, A., Larionov V., et al. 2011, Bull. Soc. Sci. Liège, 80, 361
Clark, J. S., Bartlett, E. S., Coe, M. J., et al. 2013, A&A, 560, A10
Danks, A. C., & Dennefeld, M. 1994, PASP, 106, 382
Davies, B., Figer, D. F., Kudritzki, R.-P., et al. 2007a, ApJ, 671, 781
Davies, B., Oudmaijer, R. D., & Sahu, K. C. 2007b, ApJ, 671, 2059
Davies, B., Figer, D. F., Law, C. J., et al. 2008, ApJ, 676, 1016
Davies, B., Figer, D. F., Kudritzki, R.-P., et al. 2009, ApJ, 707, 844
de Jager, C. 1998, A&ARv, 8, 145
de Jager, C., & Nieuwenhuijzen, H. 1997, MNRAS, 290, L50
Driebe, T., Groh, J. H., Hofmann, K.-H., et al. 2009, A&A, 507, 301
Egan, M. P., Price, S. D., & Gugliotti, G. M. 2001, BAAS, 34, 561
Ekström, S., Georgy, C., Eggenberger, P., et al. 2012, A&A, 537, 146
Figer, D. F., MacKenty, J. W., Robberto, M., et al. 2006, ApJ, 643, 1166
Filliatre, P., & Chaty, S. 2004, ApJ, 616, 469
Froebrich, D., & Scholz, A. 2013, MNRAS, in press [arXiv:1308.6436]
Georgy, C. 2012, A&A, 538, L8
Groh, J. H., Meynet, G., & Ekström, S. 2013a, A&A, 550, L7
Groh, J. H., Meynet, G., Georgy, C., & Ekström, S. 2013b, A&A, 558, A131
Hamann, F., Depoy, D. L., Johansson, S., & Elias, J. 1994, ApJ, 422, 626
Humphreys, R. M., Smith, N., Davidson, K., et al. 1997, AJ, 114, 2778
Humphreys, R. M., Davidson, K., & Smith, N. 2002, AJ, 124, 1026
IRAS PSC 1985, IRAS Point Source Catalogue (US Government Publ. Office)
Jones, T. J., Humphreys, R. M., Gehrz, R. D., et al. 1993, ApJ, 411, 323
Kelly, D. M., Rieke, G. H., & Campbell, B. 1994, ApJ, 425, 231
Klochkova, V G., Chentsov, E. L., & Panchuk, V. E. 1997, MNRAS, 292, 19
Klochkova, V. G., Yushkin, M. V., Chentsov, E. L., & Panchuk, V. E. 2002, Astron. Rep., 46, 139
Kochanek, C. S. 2011, ApJ, 743, 73
Koornneef, J. 1983, A&A, 128, 84
Kraus, M., Borges Fernandes, M., Kubát, J., & de Araújo, F. X. 2008, A&A, 487, 697
Kwok, S., Volk, K., & Bidelman, W. P. 1997, ApJS, 112, 557
Lagadec, E., Zijlstra, A. A., Oudmaijer, R. D., et al. 2011, A&A, 534, L10
Lobel, A., Dupree, A. K., Stefanik, R. P., et al. 2003, ApJ, 583, 923
Machado, M. A. D., de Araújo, F. X., Pereira, C. B., & Fernandes, M. B. 2002, A&A, 387, 151
Maund, J. R., Fraser, M., Ergon, M., et al. 2011, ApJ, 739, L37
Mehner, A., Baade, D., Rivinius, T., et al. 2013, A&A, 555, A116
Messineo, M., Habing, H. J., Menten, K. M., et al. 2005, A&A, 435, 575
Millour, F., Meilland, A., Chesneau, O., et al. 2011, A&A, 526, A107
Munari, U., & Tomasella, L. 1997, A&AS, 137, 521
Munari, U., Siviero, A., Bienaymé, O., et al. 2009, A&A, 503, 511
Negueruela, I., González-Fernández, C., Marco, A., Clark, J. S., & Martínez-Núñez, S. 2010, A&A, 513, A74
Negueruela, I., González-Fernández, C., Marco, A., & Clark, J. S. 2011, A&A, 528, A59
Negueruela, I., Marco, A., González-Fernández, C. et al. 2012, A&A, 547, A15
Nieuwenhuijzen, H., de Jager, C., Kolka, I., et al. 2012, A&A, 546, A105
Oksala, M. E., Kraus, M., Cidale, L. S., Muratore, M. F., & Borges Fernandes, M. 2013, A&A, 558, A17
Okumura, S., Mori, A., Nishihara, E., Watanabe, E., & Yamashita, T. 2000, ApJ, 543, 799
Oudmaijer, R. D. 1998, A&AS, 129, 541
Oudmaijer, R. D., & de Wit, W.-J. 2013, A&A, 551, A69
Oudmaijer, R. D., Geballe, T. R., Waters, L. B. F. M., & Sahu, K. C. 1994, A&A, 281, L33
Oudmaijer, R. D., Groenewegen, M. A. T., Matthews, H. E. M., Blommaert, J. A. D. L., & Sahu, K. C. 1996, MNRAS, 280, 1062
Oudmaijer, R. D., Davies, B., de Wit, W.-J., & Patel, M. 2009, ASPC, 412, 17
Ritchie, B. W., Clark, J. S., Negueruela, I., & Najarro, F. 2009, A&A, 507, 1597
Schuster, M. T., Humphreys, R. M., & Marengo, M. 2006, AJ, 131, 603
Tiffany, C., Humphreys, R. M., Jones, T. J., & Davidson, K. 2010, AJ, 140, 339
Van Dyk, S. D., Zheng W., Clubb, K. I., et al. 2013, ApJ, 772, L32
Wachter, S., Mauerhan, J. C., Van Dyk, S. D., et al. 2010, AJ, 139, 2330
Wright, E. L., Eisenhardt, P. R. M., Mainzer, A. K., et al. 2010, AJ, 140, 1868
Yamamuro, T., Nishimaki, Y., Motohara, K., Miyata, T., & Tanaka, M. 2007, PASJ, 59, 973